JURNAL SAINS MATERI INDONESIA (JUSAMI)
ISSN: 1411-1098 (print), 2614-087X (online)
VOL. 27, ISSUE 1 2025
DOI: https://doi.org/10.55981/jsmi.9988

ORIGINAL ARTICLE

Quercetin Encapsulation on Chitosan-Pectin Membranes as a Drug Delivery and Its Release Kinetics

Budi Hastuti[1*], Saptono Hadi[2], Safarin Nisriyah[1], Mutiah Martanisa[1] and Azlan Kamari[3]

[1]Department of Chemistry Education, Faculty of Teacher Training and Education, Universitas Sebelas Maret, Surakarta, Central Java, Indonesia
[2]Department of Pharmacy, Faculty of Mathematics and Natural Sciences, Universitas Sebelas Maret, Surakarta, Central Java, Indonesia
[3]Department of Chemistry, Faculty of Science and Mathematics, Universiti Pendidikan Sultan Idris, 35900, Tanjong Malim, Perak, Malaysia

ABSTRACT – Chitosan-pectin membranes are biodegradable polyelectrolyte complexes, derived from biomaterials, with good stability for drug delivery applications. This study investigates the potential of these membranes to encapsulate quercetin, a flavonoid known for its therapeutic properties but limited for its low solubility, poor bioavailability, and rapid elimination. The membranes were synthesized using a 1:1 (w/w) chitosan-to-pectin ratio and loaded with quercetin via solvent evaporation. Characterization using FTIR confirmed the presence of OH, C=O, and NH groups; XRD indicated semi-crystalline structure; and SEM revealed a uniform, porous morphology. The maximum quercetin loading efficiency reached 82.43%, with the highest release (90.39%) observed at pH 1.2, following first-order kinetics. The resulting membrane was thin, brown, homogeneous, and tear-resistant, demonstrating its potential as a controlled drug delivery matrix for quercetin.

ARTICLE HISTORY
Received: 27 Feb 2025
Revised: 11 Jun 2025
Accepted: 17 Jun 2025

KEYWORDS
Chitosan
Pectin
Quercetin

INTRODUCTION

Quercetin (Q) is one of the most abundant flavonoids found in cabbage, onions, berries, apples, red wine, broccoli, and cherries, as well as tea and red wine [1]. Currently, the pharmacokinetics of quercetin have not been fully characterized, although a number of studies have been conducted on both animals and humans [2]. However, several studies have found antioxidant, antifungal, anticarcinogenic, and hepatoprotective activity in quercetin [3].Thus, it has therapeutic potential that can treat capillary fragility, cancer [4], cardiovascular abnormalities, diabetes complications [5]. However, the benefits of quercetin in the pharmaceutical industry have limitations caused by low bioavailability, low solubility in water, low permeability, and instability [6] [7]. One way to overcome this is to use a drug delivery system in the form of a matrix that can achieve the release target so that the absorption effectiveness is high [8].

A Drug Delivery System (DDS) is a technology engineered for targeted delivery and/or controlled release of therapeutic agents. DDS controls the speed of drug release and the location of drug release in the body, some systems can control both [9]. Different systems have been developed for drug delivery, one of which includes systems that use polymers as enteric coatings, which are based on transit time or increased luminal pressure in the gastrointestinal tract, and enzymatically controlled delivery [10]. The use of this polymer-based system can be made using membranes. Polymer complexation can improve drug delivery and controlled release profiles compared to using a single polymer [11]. Polyelectrolyte complexes are complex bonds formed between oppositely charged particles. Chitosan (C) is a cationic polysaccharide obtained from the N-deacetylated base of chitin, the most abundant of the two natural polymers on earth and its polymer chain is composed of N-acetylglucosamine and glucosamine residues [12]. Pectin (P) is an anionic polysaccharide capable of providing specific colon delivery for some drugs [13]. Chitosan and pectin have anti-inflammatory, biocompatible, and biodegradable properties so that they can be combined to form membranes through the acquisition of polyelectrolyte complexes.

In this study, a complex membrane synthesis of polyelectrolytes made from chitosan-pectin will be used as a matrix carrying quercetin which will then be analyzed for the effectiveness of encapsulation and drug release from the membrane. Previous studies have shown that chitosan-pectin PEC membranes can be used as an alternative for liquid waste treatment and in the health sector [14]. In another study, thermoreversible pectin-chitosan hydrogel was able to slow down the release of drugs such as mesalamine, curcumin, and progesterone. The study showed that the release of curcumin and progesterone followed the Fickian diffusion model, while mesalamine was more in line with the second-order model. This hydrogel has the potential as a drug delivery system that can be adjusted through formulation parameters [15]. Research on the use of chitosan-pectin as a membrane for drug delivery systems is still limited, especially for quercetin compounds which have challenges in terms of stability and bioavailability.

***CORRESPONDING AUTHOR** | Budi Hastuti | ✉ budihastuti@staff.uns.ac.id

EXPERIMENTAL METHOD

Materials and Instrument

The material used is technical chitosan (CV. Ocean Fresh IPB; Bandung, Indonesia), technical equinox (CV. Nura Jaya Surabaya, Indonesia), Quercetin (Merck KgaA; Darmstadt, Germany), hydrochloric acid (HCl 32%), acetic acid (CH3COOH 2%), ethanol 96% (Merck KgaA; Darmstadt, Germany), pH buffer solutions 1.2; 5.0; and 7.4, and aquades (UNS Chemistry Sub-Laboratory; Surakarta, Indonesia).

The tools used in this study include beakers (Pyrex; Corning, USA), measuring cylinders (Pyrex; Corning, USA), stirrers, droppers, volume pipettes (Pyrex; Corning, USA), watch glasses (Pyrex; Corning, USA), magnetic stirrers, stirrers (Mtops MS300 Hs; Seoul, Korea), pH indicators, pH meters (Eutech pH 330; Illinois, USA), ovens (Memmert; Schwabach, Germany), stopwatches, analytical balances (Sartorius, d = 0.001 g; Gŏttingen, Germany), and polypropylene molds (Hawaii 550 mL; Indonesia).

Synthesis of Quercetin- loaded chitosan-pectin membrane (CPQ)

The synthesis of the CPQ membrane was carried out using a batch system with a chitosan-to-pectin (C:P) weight ratio of 1:1 (%wt). A 1:1 ratio between chitosan and pectin was used to achieve a balance of positive and negative charges, which supports the formation of stable polyelectrolyte complexes and membranes with optimal mechanical and physical properties.

First, 1.325 g of chitosan was dissolved in 25 mL of 2% (v/v) acetic acid in a beaker, and the solution was stirred using a magnetic stirrer at 1000 rpm for 30 minutes. To remove air bubbles formed during stirring, the homogeneous chitosan solution was left undisturbed overnight, covered with plastic wrap to prevent contamination.

Separately, 0.375 g of pectin was dissolved in 25 mL of 2% (v/v) acetic acid and stirred under the same conditions (1000 rpm, 30 minutes). The pectin solution was also allowed to stand overnight under similar conditions. A quercetin solution was prepared by dissolving 25 mg of quercetin in 25 mL of 96% ethanol.

After degassing, the chitosan and pectin solutions were combined in a beaker, and 1 mL of 32% hydrochloric acid (HCl) was added to the mixture. The mixture was stirred at room temperature using a magnetic stirrer at 600 rpm, while the quercetin solution was added dropwise. Stirring continued until a homogeneous solution was obtained.

The resulting CPQ mixture was then poured into a PVC mold and dried in an oven at 60 °C for approximately 24 hours to form the final membrane.

Test of Quercetin Entrapment Efficiency (%EE) on Chitosan-Pectin Membranes

200 mg of CPQ membrane was soaked in 25 mL of 96% ethanol for 24 hours. Solution absorption was measured using a UV-vis spectrophotometer with a maximum wavelength of quercetin (256.5 nm).

Clearance of Quercetin from Chitosan-Pectin Membranes

The quercetin release test from the C–P membrane was conducted using a magnetic stirrer method. Each 200 mg of CPQ membrane was placed into a beaker containing 250 mL of dissolution medium, consisting of either pure ethanol or buffer solutions at pH 1.2, 5.0, and 7.4, each mixed with ethanol in a 70:30 (buffer:ethanol, v/v) ratio. The membrane is stirrer at 75 rpm in room temperature. The release test was carried out for 4 hours, at minutes 0, 15, 30, 60, 120, 180, 240 samples were taken 5 mL each. Sample absorption is measured using a UV-vis spectrophotometer. Quercetin concentrations were quantified using a standard calibration curve. The results were calculated using zero-order equations, one-order, Higuchi and Korsmeyer-peppas models.

Membrane Characterization Test

Characterization of quercetin-loaded chitosan-pectin membranes using FTIR (Shimadzu; Kyoto, Japan), SEM (Hitachi SU3500; Tokyo, Japan) and XRD (Bruker D2 Phaser; Massachusetts, USA). Characterization using FTIR was carried out to determine the functional groups formed on the chitosan-pectin membrane. SEM characterization to determine the morphological structure of the membrane surface. XRD characterization to determine the crystallinity properties and diffraction patterns of membrane crystal structures.

RESULT AND DISCUSSION

Synthesis Membrane

The results of the synthesis of the PEC C-P membrane are shown in figure (a), the resulting membrane is brown and not easily torn. Then the C-P membrane is loaded with quercetin by using the blended membrane turned yellow (Figure b), indicating that quercetin was uniformly encapsulatedin the C-P membrane. Then the CPQ membrane is dissolved in a 96% ethanol medium to release quercetin, and a membrane with a dark brown color and a hard and rigid texture is obtained as shown in figure (c). The brown coloration likely results from the concentration and oxidation of quercetin, as well as its interaction with the chitosan–pectin matrix in an ethanol environment.

(a) (b) (c)

Figure 1. Synthesis results (a) Chitosan-Pectin membrane (b) Chitosan-Pectin-Quercetin membrane (c) Chitosan-Pectin-Quercetin Membrane after dissolution

Membrane Characterization

FTIR Characterization

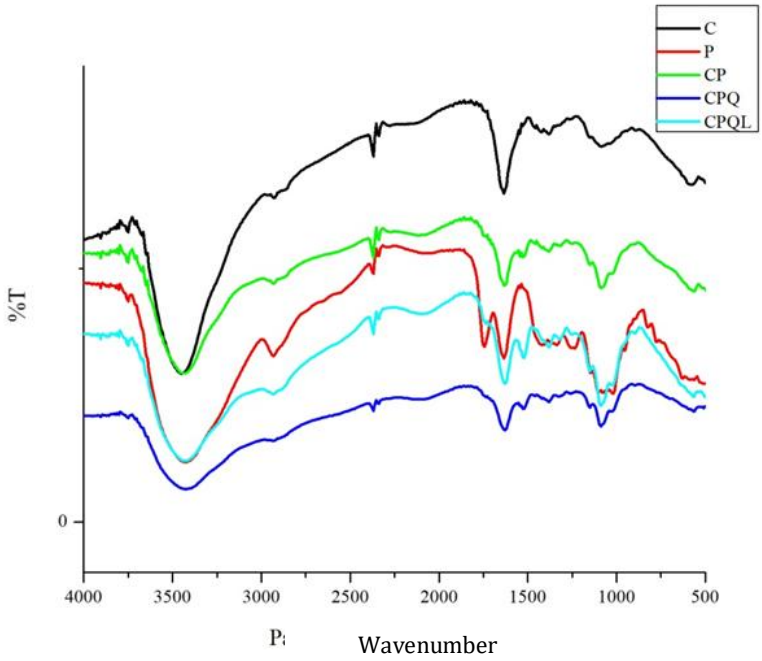

Figure 2. Results of FTIR Spectral Characterization of Chitosan-Pectin Membrane

The IR spectra of chitosan (C) and pectin (P) showed significant differences in some functional groups. The chitosan (C) spectra shows the O-H group (hydroxyl) at 3448.72 cm^{-1}, the C-H group (aliphatic) at 2931.80 cm^{-1}, and the N-H group (amine) at 1635.64 cm^{-1}. Meanwhile, the pectin (P) spectra showed the O-H group at 3425.58 cm^{-1}, the C-H group at 2931.80 cm^{-1}, as well as the stretching vibration of the C=O (carbonyl) group at 1743.65 cm^{-1} to 1635.64 cm^{-1} and the C-O group at 1018.41 cm^{-1} [16].

The chitosan-pectin (CP) membrane IR spectra showed the presence of a hydrogen bond between the O-H (hydroxyl) group of C and P with a widening and sharp peak at 3425.58 cm-1, then as a result of the electrostatic interaction between the chitosan amino group and the pectin carbonyl group appeared to peak at 1635.64 cm-1 [17]. Furthermore, the chitosan-quercetin encapsulated (CPQ) IR spectrum shows an O-H group interaction (hydroxyl) dari C, P, and Q at a peak of 3425.58 cm-1 which is wider than the spectrum of the CP membrane, the presence of an N-H group (amine) with a peak at 1627.92 cm-1, a stretch at wave number 1381.03 cm-1 showing the aromatic ring of quercetin of the phenolic part of the quercetin molecule, and bands at 1257.59 cm-1 and 1087.85 cm-1 caused by the conjugation of aryl ether with C=C-O of the aromatic ring of quercetin, this suggests that quercetin is well encapsulated in the CP membrane [18]. Furthermore, the IR spectra of the quercetin-encapsulated chitosan-pectin membrane after release or solution through 96% ethanol medium (CPQL) showed a widening of the peak of the hydroxyl group from 3425 cm-1 which showed that the hydroxyl group derived from quercetin had been released even though it was not optimal, and there was no release of other active groups as evidenced by the peak at 1627.92 cm-1 which indicates the presence of amine groups, and the peak at 1087.85 cm-1 indicates the presence of C-O groups [19].

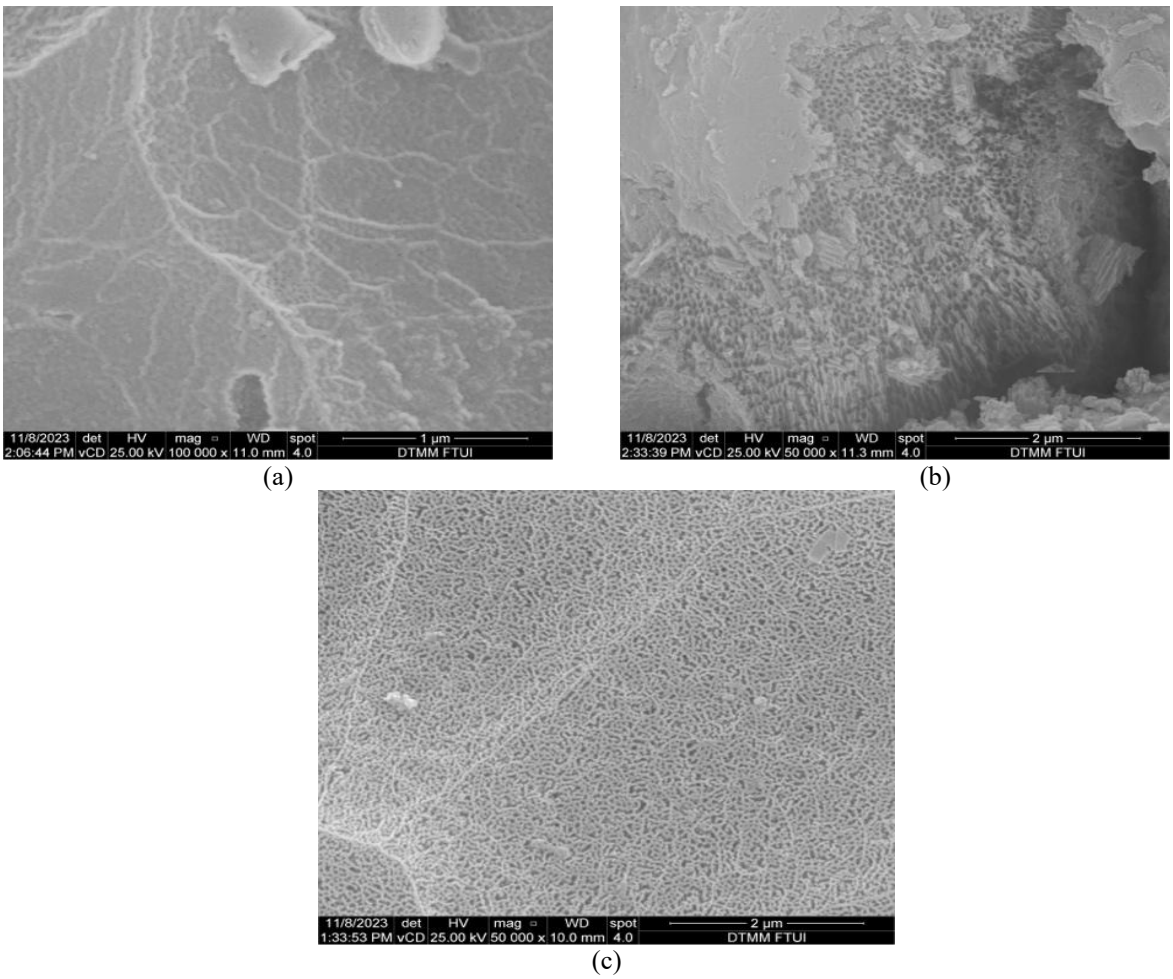

Figure 1. FE-FEM surface morphology of the AAO layer after the anodizing process in the electrolyte of a) 0.3 M, b) 0.5 M, and c) 0.7 M oxalic acid for 3 h at room temperature and the voltage of 30 V

In accordance with the chemical composition analyzed through EDX spectroscopy (Table 1), the anodized layer is predominantly composed of oxygen and aluminum in the Al_2O_3 stoichiometry.

Table 1. Weight and Atomic composition of the AAO layers grown by 3 h anodizing process at 30 V in various electrolytes, as deduced from EDX analysis

	Al (wt%)	O (wt%)	Al (at%)	O (at%)
0.3 M Oxalic Acid	53.69	46.31	40.74	59.26
0.5 M Oxalic Acid	50.45	35.85	41.32	49.52
0.7 M Oxalic Acid	55.36	44.64	42.38	57.62

Table 1 also indicates that there is a difference between concentrations of oxygen in the AAO layer produced by different anodizing parameters. The amount of oxygen content in the specimens conducted to the anodizing process of 0.3 M and 0.7 M oxalic acid remains the same. The AAO layer contains 46.31 wt% and 44.64 wt% of oxygen for 0.3 M and 0.7 M oxalic acid, respectively. The lowest oxygen percentage, about 35 wt%, was found in the AAO layer formed in the anodizing parameter of 0.5 M oxalic acid. This phenomenon accounts for the morphology of cylindrical nanopores in accordance with the FE-SEM image in Figure 1.

Ni Coating Morphology

In this study, the electroless Ni-P deposition was conducted directly on AAO interlayers without the existence of a surface activation agent.

Fig. 2 illustrates the FE-SEM surface morphology of the coatings after Ni-P deposition on the anodized layer. The images clearly show the deposit of nickel nodules with a size in the order of 0.5 μm or less for all anodizing electrolytes studied. It could be observed that the AAO surface is covered by a thin and tightly formed layer of nickel. During the electroless deposition process, nickel ions infiltrate the pores of the anodized layer and initiate reduction there. The deposited nuclei then serve as catalytic sites for further nickel phosphorus deposition, as described by Backovic et al.[35]. Gutzeit [36] proposed that the nickel ion undergoes catalytic reduction through active atomic hydrogen, resulting in the simultaneous formation of orthophosphite and hydrogen ions. Moreover, Khan et al. [8] proposed that the catalytic dehydrogenation of adsorbed hypophosphite molecules on the surface leads to the release of atomic hydrogen, which subsequently reduces nickel at the catalyst surface. However, for all anodizing electrolytes studied, the electroless deposited Ni-P coatings directly applied to AAO exhibit inferior qualities including cracks. This phenomenon can be attributed to the failure of nickel cations to easily move through the pores of the anodized layer[1].

EDX analysis was carried out to investigate the coverage of Ni-P coating and to determine the composition of nickel and other elements during electroless nickel deposition onto AAO on the AA5052 surface at an immersion time of 60 min, room temperature, and pH 5 as shown in Table 2. As can be seen in Table 2, the percentage of oxygen after Ni deposition in all anodizing parameters decreases up to 70% compared to the amount of oxygen in Table 1. This phenomenon indicates that Ni deposits can cover the surface of AAO on the AA5052 substrate. Therefore, the oxygen accessibility to the AAO surface can be diminished by this layer. On the other hand, the increase in the percentage of aluminum (Al) can be attributed to the displacement of a portion of the surface oxide during the deposition process.

With respect to the nickel concentration in the coatings, the AAO retains the potential to serve as catalytic sites for nickel deposition, albeit with the formation of a thin Ni coating. Moreover, it could be observed that the nickel content slightly decreases with the increase in the concentration of oxalic acid from 0.3 M to 0.7 M. It can be associated with the surface morphology of AAO, as seen in Fig. 1. It is evident that the surface of AAO conducted from the anodizing process in 0.3 M oxalic acid is smoother than that of in the 0.5 and 0.7M oxalic acids. Therefore, the formation of nickel coating on this AAO interlayer is thicker. In brief, the presence of uniform and smooth surfaces of AAO interlayer provides more effective sites for the deposition of nanoparticles of nickel coatings.

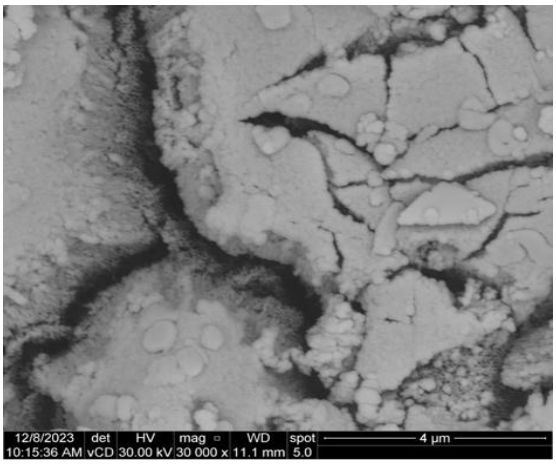

(a)

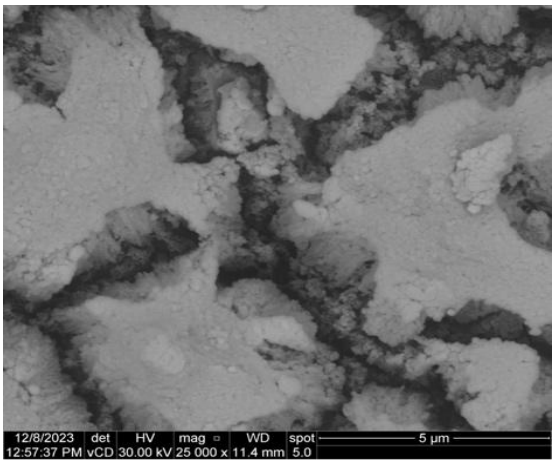

(b)

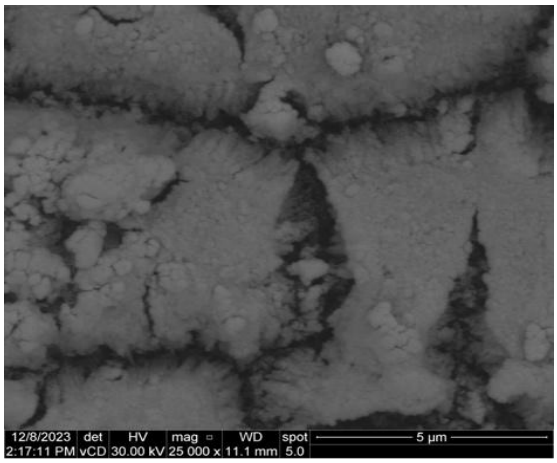

(c)

Figure 2. FE-FEM surface morphology of the AAO layer after the anodizing process in the electrolyte of a) 0.3 M, b) 0.5 M, and c) 0.7 M oxalic acid for 3 h at room temperature and the voltage of 30 V

Table 2. Weight and Atomic composition of the AAO layers grown by 3 h anodizing process at 30 V in various electrolytes, as deduced from EDX analysis

	Al (wt%)	O (wt%)	Ni (wt%)
0.3 M + NiP	72.49	13.70	08.27
0.5 M + NiP	69.89	19.40	06.65
0.7 M + NiP	78.18	15.95	05.87

CONCLUSION

In this study, in order to investigate the impact of electrolyte solution concentration during the anodizing process on the Ni-P; deposition results, the coating of Ni-P on Anodic Aluminum Oxide (AAO) was applied to the surface of aluminum AA5052 specimens with the absence of a surface activation agent. The AAO interlayer formed by an anodizing process in 0.3,0.5, and 0.7 M oxalic acid. The primary conclusions are listed below:

- AAO produced by anodizing in 0.3M oxalic acid exhibited a crater-like structure with well-defined boundaries and small holes located within the craters. The 0.5 M oxalic acid anodized specimen displayed cylindrical nanopores that resembled hexagonal cells. Moreover, an anodized specimen of 0.7 M oxalic acid exhibited a structural transformation from a nanoporous to a "mesh" configuration.
- The results of Ni-P coating for all anodizing parameters indicate the formation of nickel nodules with a diameter of 0.5 μm or smaller on the AAO surface. Nevertheless, the electroless deposited Ni-P coatings that were applied directly to AAO demonstrated inferior qualities including cracks.

Moreover, the nickel content exhibits a gradual reduction when the concentration of oxalic acid increases from 0.3 M to 0.7 M. It was found that the best arrangement for Ni-P deposition on anodized AA5052 was obtained for an oxalic acid concentration of 0.3 M.

ACKNOWLEDGEMENT

The studies and analysis were performed with the financial support of the International Collaboration Research Grant, Politeknik Negeri Jakarta No. 385/PL3.A.10/PT.00.06/2024 on 25th April 2024.

REFERENCES

[1] A. F. Almeida *et al.*, "Bioavailability of Quercetin in Humans with a Focus on Interindividual Variation," *Compr. Rev. Food Sci. Food Saf.*, vol. 17, no. 3, pp. 714–731, 2018, doi: 10.1111/1541-4337.12342.

[2] D. Xu, M. J. Hu, Y. Q. Wang, and Y. L. Cui, "Antioxidant activities of quercetin and its complexes for medicinal application," *Molecules*, vol. 24, no. 6, 2019, doi: 10.3390/molecules24061123.

[3] G. El-Saber Batiha *et al.*, "The pharmacological activity, biochemical properties, and pharmacokinetics of the major natural polyphenolic flavonoid: Quercetin," *Foods*, vol. 9, no. 3, 2020, doi: 10.3390/foods9030374.

[4] A. J. Vargas and R. Burd, "Hormesis and synergy: Pathways and mechanisms of quercetin in cancer prevention and management," *Nutr. Rev.*, vol. 68, no. 7, pp. 418–428, 2010, doi: 10.1111/j.1753-4887.2010.00301.x.

[5] K. M. Krishna *et al.*, "Partial reversal by rutin and quercetin of impaired cardiac function in streptozotocin-induced diabetic rats," *Can. J. Physiol. Pharmacol.*, vol. 83, no. 4, pp. 343–355, 2005, doi: 10.1139/y05-009.

[6] J. Maciej *et al.*, "Bioavailability of the flavonol quercetin in neonatal calves after oral administration of quercetin aglycone or rutin," *J. Dairy Sci.*, vol. 98, no. 6, pp. 3906–3917, 2015, doi: 10.3168/jds.2015-9361.

[7] G. T. Rich, M. Buchweitz, M. S. Winterbone, P. A. Kroon, and P. J. Wilde, "Towards an understanding of the low bioavailability of quercetin: A study of its interaction with intestinal lipids," *Nutrients*, vol. 9, no. 2, 2017, doi: 10.3390/nu9020111.

[8] H. Patel, D. R. Panchal, U. Patel, T. Brahmbhatt, and M. Suthar, "Matrix Type Drug Delivery System : A Review," *J. Pharm. Sci. Biosci. Res.*, vol. 1, no. 3, pp. 143–151, 2011.

[9] G. Tiwari *et al.*, "Drug delivery systems: An updated review," *Int. J. Pharm. Investig.*, vol. 2, no. 1, p. 2, 2012, doi: 10.4103/2230-973x.96920.

[10] G. F. Oliveira, P. C. Ferrari, L. Q. Carvalho, and R. C. Evangelista, "Chitosan-pectin multiparticulate systems associated with enteric polymers for colonic drug delivery," *Carbohydr. Polym.*, vol. 82, no. 3, pp. 1004–1009, 2010, doi: 10.1016/j.carbpol.2010.06.041.

[11] M. R. I. Shishir, N. Karim, V. Gowd, J. Xie, X. Zheng, and W. Chen, "Pectin-chitosan conjugated nanoliposome as a promising delivery system for neohesperidin: Characterization, release behavior, cellular uptake, and antioxidant property," *Food Hydrocoll.*, vol. 95, pp. 432–444, 2019, doi: https://doi.org/10.1016/j.foodhyd.2019.04.059.

[12] M. George and T. E. Abraham, "Polyionic hydrocolloids for the intestinal delivery of protein drugs: Alginate and chitosan - a review," *J. Control. Release*, vol. 114, no. 1, pp. 1–14, 2006, doi: 10.1016/j.jconrel.2006.04.017.

[13] F. Bigucci, B. Luppi, L. Monaco, T. Cerchiara, and V. Zecchi, "Pectin-based microspheres for colon-specific delivery of vancomycin," *J. Pharm. Pharmacol.*, vol. 61, no. 1, pp. 41–46, 2008, doi: 10.1211/jpp/61.01.0006.

[14] N. P. S. Ayuni, D. Siswanta, and A. Suratman, "SINTESIS DAN KARAKTERISASI MEMBRAN KOMPLEKS POLIELEKTROLIT (PEC) KITOSAN-PEKTIN Ni Putu Sri Ayuni 1 , Dwi Siswanta 2 , Adhitasari Suratman 2," *J. Wahana Mat. dan Sains*, vol. 8, no. April, pp. 88–96, 2014.

[15] L. Neufeld and H. Bianco-Peled, "Pectin–chitosan physical hydrogels as potential drug delivery vehicles," *Int. J. Biol. Macromol.*, vol. 101, pp. 852–861, 2017, doi: 10.1016/j.ijbiomac.2017.03.167.

[16] J. M. Joel, J. T. Barminas, E. Y. Riki, J. M. Yelwa, and F. Edeh, "Extraction and Characterization of Hydrocolloid Pectin from Goron Tula (Azanza garckeana) fruit," *World Sci. News*, vol. 101, no. June, pp. 157–171, 2018.

[17] A. S. Soubhagya, A. Moorthi, and M. Prabaharan, "Preparation and characterization of chitosan/pectin/ZnO porous films for wound healing," *Int. J. Biol. Macromol.*, vol. 157, pp. 135–145, 2020, doi: 10.1016/j.ijbiomac.2020.04.156.

[18] I. C. C. M. Porto, T. G. Nascimento, J. M. S. Oliveira, P. H. Freitas, A. Haimeur, and R. França, "Use of polyphenols as a strategy to prevent bond degradation in the dentin-resin interface.," *Eur. J. Oral Sci.*, vol. 126, no. 2, pp. 146–158, Apr. 2018, doi: 10.1111/eos.12403.

[19] A. B. D. Nandiyanto, R. Oktiani, and R. Ragadhita, "How to read and interpret ftir spectroscope of organic material," *Indones. J. Sci. Technol.*, vol. 4, no. 1, pp. 97–118, 2019, doi: 10.17509/ijost.v4i1.15806.

[20] P. Mukhopadhyay *et al.*, "Oral delivery of quercetin to diabetic animals using novel pH responsive carboxypropionylated chitosan/alginate microparticles," *RSC Adv.*, vol. 6, no. 77, pp. 73210–73221, 2016, doi: 10.1039/c6ra12491g.

[21] P. Mukhopadhyay *et al.*, "Oral delivery of quercetin to diabetic animals using novel pH responsive carboxypropionylated chitosan/alginate microparticles," *RSC Adv.*, vol. 6, no. 77, pp. 73210–73221, 2016, doi: 10.1039/C6RA12491G.

[22] N.-Q. Shi, Y.-S. Lei, L.-M. Song, J. Yao, X.-B. Zhang, and X.-L. Wang, "Impact of amorphous and semicrystalline polymers on the dissolution and crystallization inhibition of pioglitazone solid dispersions," *Powder Technol.*, vol. 247, pp. 211–221, 2013, doi: https://doi.org/10.1016/j.powtec.2013.06.039.

[23] N. S. Heredia *et al.*, "Comparative statistical analysis of the release kinetics models for nanoprecipitated drug delivery systems based on poly(lactic-co-glycolic acid)," *PLoS One*, vol. 17, no. 3 March, 2022, doi: 10.1371/journal.pone.0264825.

[24] M. P. Paarakh, P. A. N. I. Jose, C. M. Setty, and G. V Peter, "Release Kinetics – Concepts and Applications," *Int. J. Pharm. Res. Technol.*, vol. 8, no. 1, pp. 12–20, 2019, doi: 10.31838/ijprt/08.01.02.

[25] S. Rochín-Wong *et al.*, "Drug release properties of diflunisal from layer-by- layer self-assembled k-carrageenan/chitosan nanocapsules: Effect of deposited layers," *Polymers (Basel).*, vol. 10, no. 7, pp. 1–16, 2018, doi: 10.3390/polym10070760.

[26] R. K.H, D. P.A, K. A.R, and P. S.V, "Kant's biological conception of history," *J. Philos. Hist.*, vol. 3, no. 5, pp. 388–396, 2014, doi: 10.1163/187226308X268845.

[27] S. Dwi, H. Fithriya, O. Heni, and Mudasir, "Chitosan-pectin-stearic acid film for controlled-release of curcumin," *Mater. Sci. Forum*, vol. 948 MSF, pp. 69–77, 2019, doi: 10.4028/www.scientific.net/MSF.948.69.

[28] Y.N Martinez, L. Piñuel, G.R.Castro, and J.D. Breccia "Polyvinyl alcohol-pectin cryogel films for controlled release of enrofloxacin" *Appl Biochem Biotechnol*., vol. 167, pp. 1421–1429, 2012, doi.org/10.1007/s12010-012-9554-6

[29] M. Ferrante, A. Vera, Alvarez, B. Liesel, Gede, D. Guerrieri, E. Chuluyan and S. Jimena, Gonzalez. "Polyelectrolyte complexes hydrogels based on chitosan/pectin/NaCl for potentially wound dressing: development, characterization, and evaluation", *Colloid and Polym Sci.,* vol. 302, pp 1231–1245, 2024doi.org/10.1007/s00396-024-05261-y

[30]. B. Boruah, P.M. Saikia, and R.K. Dutta, "Binding and stabilization of curcumin by mixed chitosan-surfactant systems: A spectroscopic study", *J. of Photochem and Photobio A: Chemistry*, vol. *245*, pp. 18–27, 2012, https://doi.org/10.1016/j.jphotochem.2012.07.004

[31] S. Dey and K. Sreenivasan, (). Conjugation of curcumin onto alginate enhances aqueous solubility and stability of curcumin. *Carbohydrate Polym*., vol.. *99*, pp. 499–507, 2014, doi.org/10.1016/j.carbpol.2013.08.067